COMMUNICATION

Check for updates

A single-layer Janus membrane with dual gradient conical micropore arrays for self-driving fog collection†

Feifei Ren,[a] Guoqiang Li,[bc] Zhen Zhang,[b] Xuedong Zhang,[a] Hua Fan,[d] Chen Zhou,[e] Yulong Wang,[b] Yinghui Zhang,[b] Chaowei Wang,[b] Kai Mu,[f] Yahui Su*[a] and Dong Wu (ID) *[b]

Inspired by natural creatures, the development of a device that collects water from fog represents an important research direction. However, present methods suffer from low efficiency, complex processes, expensive materials, *etc.* In this study, a single-layer hydrophilic/hydrophobic heterogeneous Janus aluminum membrane based on dual gradient conical micropore arrays is designed and fabricated by laser drilling and subsequent low surface energy modification. The droplets can automatically pass through the conical micropores on the Janus membrane, which results from the wetting driving force of gradient surface energy and the Laplace pressure of the conical morphology. Compared to the superhydrophilic membranes, the Janus membrane possesses a 209% enhancement in the water collection efficiency. This new type of self-driving water collection membrane may offer a way to construct an efficient fog collection system to relieve the freshwater crisis.

Introduction

In recent years, fog collection by surface microstructures possessing special wettability has attracted great attention due to growing water shortage with the development of society.[1–13]

[a]School of Electrical Engineering and Automation, Anhui University, Hefei, Anhui, 230601, P. R. China. E-mail: ustcsyh@ahu.edu.cn

[b]CAS Key Laboratory of Mechanical Behavior and Design of Materials, Department of Precision Machinery and Precision Instrumentation, University of Science and Technology of China, Hefei, Anhui, 230026, P. R. China. E-mail: dongwu@ustc.edu.cn

[c]Key Laboratory of Testing Technology for Manufacturing Process of Ministry of Education, Southwest University of Science and Technology, Mianyang, Sichuan, 621010, P. R. China

[d]School of Mechanical Engineering, Hefei University of Technology, Hefei, Anhui, 230009, P. R. China

[e]School of Instrument Science and Opto-electronics Engineering, Hefei University of Technology, Hefei, Anhui, 230009, P. R. China

[f]Department of Modern Mechanics, University of Science and Technology of China, Hefei, Anhui, 230026, P. R. China

† Electronic supplementary information (ESI) available: ESI Fig. S1–S5 and Movies S1–S4. See DOI: 10.1039/c7ta04392a

Inspired by nature, various bionic structures and functional devices, such as the bump-like structure of Namib desert beetles' back[2,14–16] and the spindle-knots structure of spider silk,[5–8,17,18] have been fabricated for collecting fog. Hou *et al.* proposed a hybrid surface with patterned high-contrast wettability to achieve a 63% enhancement compared to the conventional dropwise condensation on the flat hydrophobic silicon surface.[14] Bai *et al.* fabricated a series of bioinspired artificial spider silks (BASs) with controllable spindle-knot geometry that showed a high efficient fog collection ability.[5,7,8,17]

Based on previous research, scientists have found some necessary features for constructing efficient fog collectors:[9] (1) a relatively hydrophobic surface; (2) continuous generation of fresh surface; (3) lower re-evaporation rate of collected water; and (4) rapid transport of surface water. Consequently, most effective strategies to collect and preserve water are based on the hierarchical structures with complementary hydrophobic/hydrophilic wetting on the opposite surfaces.[9] Therefore, researchers have proposed a type of special Janus surface with asymmetrical wettability.[1,9,19–25] On one side (outside) of the material surface, its wetting state is superhydrophobic for collecting fog, whereas on the other (inside) side, its wetting state is superhydrophilic for preserving the collected water. For example, Cao *et al.* reported a hydrophobic/hydrophilic heterogeneous Janus system consisting of two types of different materials – cotton absorbent and modified copper mesh that achieved 130% improvement in fog collection.[9]

In this study, we reported a facile single-layer hydrophobic/hydrophilic Janus aluminum membrane with conical micropore arrays for efficient fog collection that was fabricated by femtosecond laser drilling[11,26] and subsequent selective surface modification. Compared with superhydrophilic membranes, the Janus membrane showed 209% enhancement in fog collection. The dynamic process of fog collection was *in situ* monitored, and the physical mechanism was systemically investigated. This study provides new insights on the hydrophobic/hydrophilic Janus membrane with high efficiency fog collection, which will be beneficial for their practical applications.

This journal is © The Royal Society of Chemistry 2017

J. Mater. Chem. A, 2017, 5, 18403–18408 | 18403

Experimental

The aluminum foil purity is more than 99.5%, and the thickness is 35 μm. The superhydrophilic membrane consists of uniform conical micropore arrays drilled with a distance of 100 μm and diameters of 10, 20, 30, and 40 μm by adjusting the laser pulse energy and pulse number using a regenerative amplified Ti:sapphire femtosecond laser system (Legend Elite-1K-HE, Coherent, USA, 104 fs, 1 kHz, 800 nm). The superhydrophobic membrane was fabricated by modifying the superhydrophilic membrane with a 1.0% ethanol solution of 1H,1H,2H,2H-per-fluorodecyltriethoxysilane (PFDTES) at room temperature for 24 hours. The Janus membrane was prepared by laser scanning to remove the PFDTES-modified material of the bottom surface on the superhydrophobic membrane.

The contact angles of 5 μL of water were measured using a contact-angle system (CA100D, Innuo, China), and the average values were obtained by measuring five drops at different locations. Surface morphology was exhibited by a field-emission scanning electron microscope (JSM-6700F, JEOL, Tokyo, Japan). The dynamic process where the droplet (5 μL) penetrated through the membrane was recorded with a high-speed video camera (FASTCAM SA6, Photron, USA).

Fog collection experiment

The as-prepared sample membranes with a hole diameter from 10 to 100 μm and distance from 50 to 500 μm (the area of micropores were the same) were fixed at 5 cm below the nozzle of humidifier. The fog flow had a velocity of 70 cm s^{-1}. For comparing the efficiency of membranes, three 3 cm × 3 cm samples (the diameters are 30 μm, and the distances are 100 μm) were used to collect water, employing a funnel and cylinder. One milliliter of water dyed blue with methylene blue was put in the cylinder beforehand.

Permeation pressure measurement

The as-prepared sample was invertedly fixed between two glass vessels with a diameter of 10 mm at 25 °C. The pressure value was recorded when water began to penetrate the membrane.

Results and discussion

The aluminum foil with oxide layer is one of the most widely used materials in commercial applications due to its numerous advantages including strong oxidation resistance, good plasticity, and cost efficiency. The fabrication process of a Janus membrane is illustrated in Fig. 1a–c. In order to better distinguish two sides of the membrane, we named the laser-incident surface as the bottom surface and the opposite side as the top surface. The micropore diameter and the distance between two adjacent pores were set at 30 and 100 μm, respectively. The water contact angles (WCA) of flat and the drilled aluminum foil (superhydrophilic membrane) were ∼57° and 2°, respectively. After low surface energy modification, both the WCA of bottom and top surfaces increased to 155° (superhydrophobic membrane) (Fig. S1†). For the Janus membrane, the measured

WCA of the bottom surface was ∼8°. On the contrary, the WCA of the top surface changed from 156° to 0° gradually, and the dynamic process is shown in Fig. 1d. It is indicated that the droplet remains in a hydrophobic state from the beginning to 0.315 s and then suddenly perforates the Janus membrane in less than 0.048 s (Movie S1†). In order to better analyze the suction process, the dynamic contact angle and dynamic contact line with diameters of 10, 20, 30, and 40 μm were also systematically studied, which verify that all the phenomena are similar to the case described above (Fig. S2†).

To explain this phenomenon, the morphology of the micropore was investigated. Fig. 2a and b and S3† display the scanning electron microscope (SEM) images of the Janus aluminum membrane with top and bottom views. The obconical micropore arrays exhibited rough circular morphology on the bottom layer and relative flat one on the other side. From the insets in Fig. 2a and b, it is seen that the top and bottom diameters are 29.6 and 42.1 μm, respectively. In addition, the morphology in the inner conical pore is also studied as exhibited in Fig. 2c–e and S4,† from which we can see that mastoids on the lower side are bigger than that on the upper one. The generation of conical micropores is benefited by lens focusing characteristics of a cone-shaped focused laser spot and Gaussian power distribution. Therefore, the structure of the entire conical micropore can be divided into three components: top surface, conical pore, and bottom surface. The phenomenon that the droplet would flow toward the inner micropore and then transfer to the opposite surface was explained by wetting difference and conical morphology.

First, the increased wetting from the top surface to the bottom one can be described using the Wenzel model as shown in eqn (1):

$$\cos \theta'_{WA} = r \cos \theta_{WA} \tag{1}$$

In our case, r represents roughness, and θ_{WA} and θ'_{WA} are intrinsic and practical water contact angles. The PFDTES-modified micropore arrays make the top surface more hydrophobic, whereas the relatively rough micropore arrays make the laser-scanning bottom surface more hydrophilic. Comparatively, the structures inside the conical micropore are more complicated. On one hand, the roughness differences make the lower area more hydrophilic. On the other hand, a possible reason is that the difference of laser energy along the optical axis direction leads to a gradient of residual PFDTES-modified material, which enhances the entire difference of wettability on the inner surface of the micropore. Hence, the difference of surface-free energy produces a wetting driving force $T_{wet-force}$, which drives the water drops collected on the top of conical pores to directionally penetrate towards the bottom of conical pores. The model can be described as follows:[1,4,27]

$$T_{wet-force} = \cos \frac{\varphi}{2} \int_{\theta_{top}}^{\theta_{bottom}} -2\pi R \times \gamma \times \sin \theta d\theta \tag{2}$$

where φ, γ, R, θ_{bottom} and θ_{top} are the tip angle of conical micropore, water surface tension, the local radius of conical micropore, and the water contact angles on the bottom and top
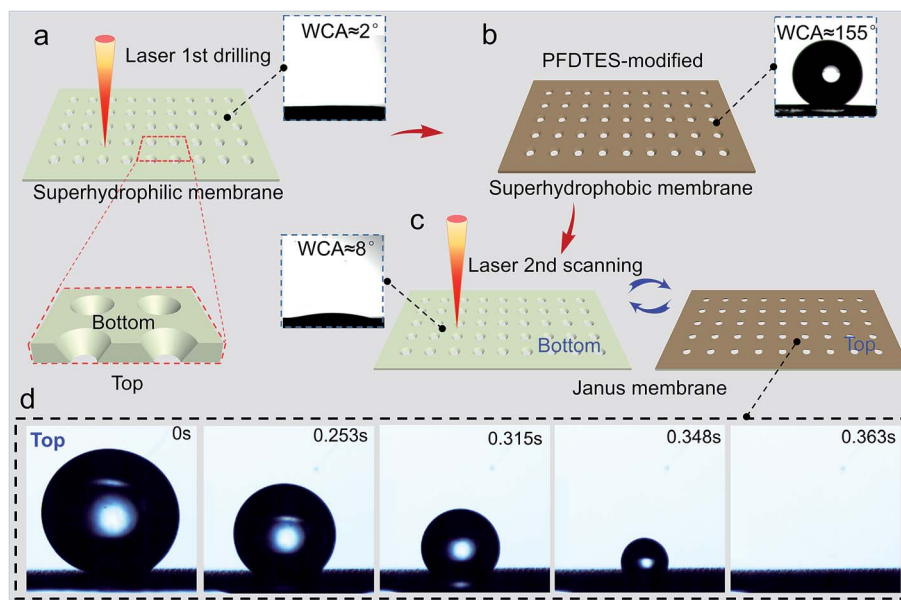
Fig. 1 The schematic diagram shows fabrication and characteristics of the Janus membrane. (a) The regular micropore arrays on ultrathin aluminum foil are drilled by a femtosecond laser, and the WCA (superhydrophilic membrane) is ~2°. (b) The drilled membrane was modified with 1H,1H,2H,2H-perfluorodecyltriethoxysilane (PFDTES), and the WCA is ~155° (superhydrophobic membrane). (c) The Janus membrane was fabricated by scanning the bottom layer of the superhydrophobic membrane by laser, and the WCA of the bottom surface is ~8°. (d) The dynamic process where the droplet was absorbed from the top surface to the bottom surface.
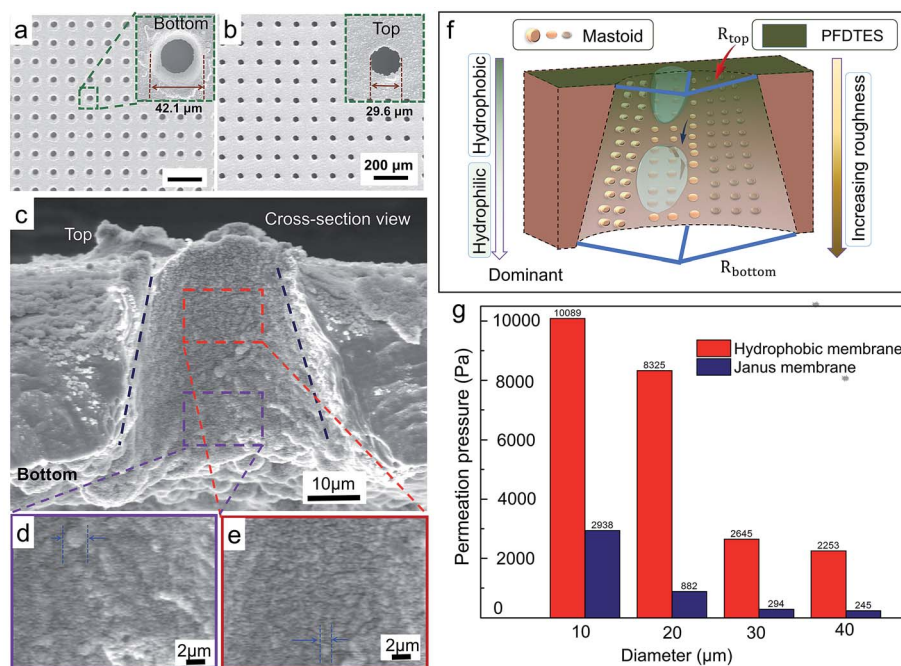

Fig. 2 (a, b) The SEM images of Janus membrane's bottom and top surface. (c) The cross-section view of a conical pore. (d, e) The SEM images of top and bottom areas in the conical pore. (f) The schematic diagram of Laplace pressure ($\Delta F_{\text{Laplace}}$) and wetting gradient driving force ($T_{\text{drive-force}}$). (g) The permeation pressure calculated by the heights of affordable water on the superhydrophobic membrane and Janus membrane with different diameters.

of conical micropores, respectively. The values of γ, θ_{bottom} and θ_{top} are estimated to be 7.2×10^{-2} N m^{-1}, 150 and 10°, respectively. Hence the wetting driving force ($T_{\text{wet-force}}$) is

roughly estimated to be ~1.4919×10^{-5} N when the conical micropore is filled with water.

In addition, the gradient wetting in the conical pore makes the water show different states at the bottom and top area of the

inwall, which is the reason for the suction, as well. The water shape is hemispherical at the tip of the conical micropores and flat at the base of the conical micropores when the conical micropore is filled with water. The Laplace pressure can be described as follows:[1,4,12,13,28,29]

$$\Delta F_{Laplace} = \pi R^2 \times \gamma \times \frac{2}{R_{top}} \qquad (3)$$

where R, R_{top}, and γ are the base radius of the sphere, droplet surface radius in the top area of the inner conical pore and the surface tension of water, respectively; their values are 1.5×10^{-5} m, 2.0×10^{-5} m and 7.2×10^{-2} N m^{-1}, respectively. The Laplace pressure ($\Delta F_{Laplace}$) is roughly estimated to be 5.089×10^{-6} N. The model of self-driving force ($F_{self-drive} = \Delta F_{Laplace} + T_{wet-force}$) is illustrated in Fig. 2f. In order to verify the value of the suction pressure, the maximum height of the water layer that can be supported on the superhydrophobic membrane and Janus membrane was measured, which would be explained by eqn (4):

$$P_{per} = \rho_w g h_{max} \qquad (4)$$

where ρ_w, g and h_{max} are the density of water, the gravity acceleration, and the maximum height of the water layer that the membrane can support, respectively. The obtained h_{max} values are 3 and 27 cm for the Janus membrane and superhydrophobic membrane, and the calculated penetration pressures are 294 and 2645 Pa, respectively. In addition, the self-driving pressure (P_{per}) is equal to the penetration pressure, which is approximately 2.94×10^{-6} N per pore (Fig. 2g).

Fog collection experiment was conducted to analyze the fog collection ability of the Janus aluminum membrane, which was also compared with superhydrophilic and superhydrophobic ones (Movies S2 and S3†). For the superhydrophilic membrane, the water drops adhered in a spherical shape when they impacted the surface. Then, the water droplets rapidly spread and penetrated the aluminum membrane. As a result, both sides of the membrane and the inside of the micropores were filled with water in a very short time (Fig. 3a). When the fog flow contacted with the superhydrophobic membrane surface, some of the water drops adhered to the surface, while most of water drops jumped and deviated from the membrane. The adhered droplets were coalesced with subsequent ones, and then coalesced droplets jumped, resulting from the surface energy released upon drop coalescence. Finally, both sides of the membrane remained dry, as illustrated in Fig. 3b, where the red arrow indicates the droplet growing, and the yellow arrow shows a jumped droplet.

Comparatively, the Janus membrane demonstrated a unique way to harvest water. The water drops easily adhered to the surface with the fog flow, coalesced with subsequent water drops, and then grew even more. The droplets can enter into the conical micropores once they are contacted with the micropore edge due to the driving force ($F_{self-drive}$) and then are transferred to the opposite surface in a very short time. The size of the remaining droplet on the top surface is not larger than 80 µm even after ten minutes. In this way, the top surface can maintain a dry state, while the bottom surface is in a wetted state, thus
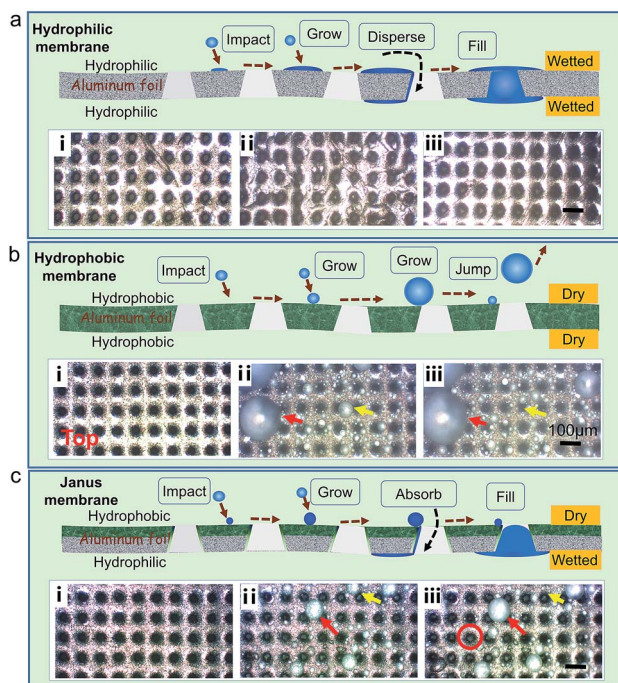

Fig. 3 The fog collection behaviors of superhydrophilic membrane, superhydrophobic membrane and Janus membrane. For superhydrophilic membrane (a), the water drops would be adhered as a spherical shape when it just impacted the surface and then penetrated the aluminum membrane. For superhydrophobic membrane (b), some of the water drops were adhered to the surface, while most of water drops jumped and deviated from the membrane; the red arrow indicates the droplet growing, while the yellow arrow shows a jumped droplet. For the Janus membrane (c), the water drops were easily adhered to the surface, coalesced with subsequent water drops, and then grew up. The droplets can enter into the conical micropores once they contacted the micropore edge due to the driving force and then were transferred to the opposite surface in a very short time. The red and yellow arrows show a growing droplet and an absorbed one.

exhibiting ∼75% decreased re-evaporation rate of collected water, which is associated with the ratio between area of micropores and membrane (25%). This is illustrated in Fig. 3c, where the yellow arrow indicates the droplet absorbed, and the red arrow shows the growing one.

A fog collection system was designed to further verify the collection ability of a Janus membrane. As shown in Fig. 4a, 0, 1.8, and 4.6 mL of water were collected by the superhydrophobic membrane, superhydrophilic membrane, and Janus membrane, respectively, after 8 minutes. After 15 minutes, 0.1, 3.9, and 8.1 mL of water could be collected. The average collection rates of three types of membranes are 0, 0.022, and 0.068 mL min^{-1} cm^{-2}. It can be observed that the Janus membrane has the highest collection rates compared with the superhydrophobic membrane and superhydrophilic membrane, and the improvement can reach up to 209% compared with the superhydrophilic membrane (Fig. 4b, Movie S4†).

In addition, the fog collection rates with different diameters and same micropore area in one sample were also systematically studied (Fig. S5†). The collection rates increased from 0.04 to 0.05 and then decreased to 0.03 cm^{-2} min^{-1} as the diameters

18406 | J. Mater. Chem. A, 2017, 5, 18403–18408

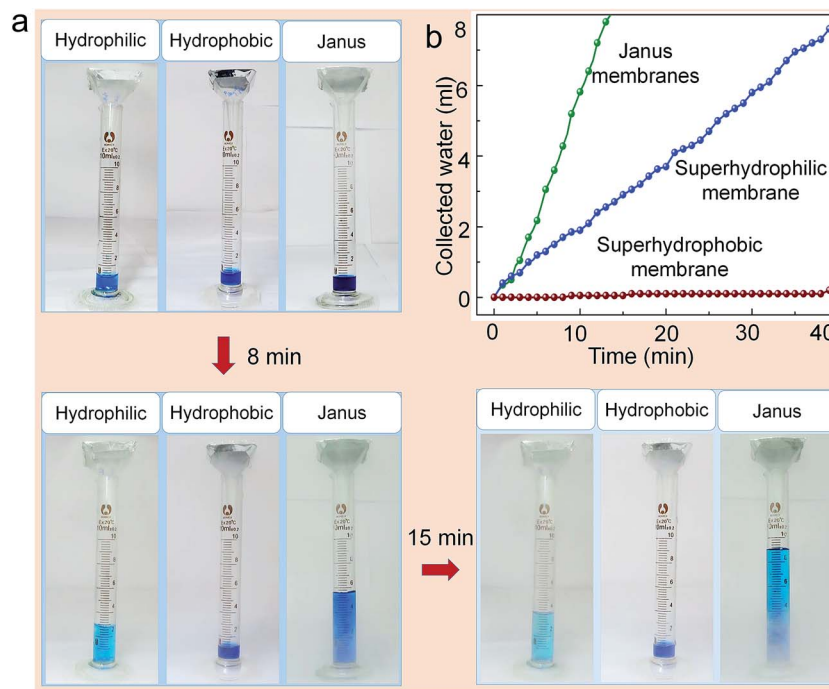This journal is © The Royal Society of Chemistry 2017

Fig. 4 (a) The fog collection system at 0, 8, and 15 min. (b) The fog collection ability of the Janus membrane compared with two kinds of wetting membranes. The Janus membrane shows considerable enhancement with the collection efficiency.

increased from 10 to 100 μm. Therefore, the optimal diameter of fog collection was 20 μm, which could reach 0.05 g cm^{-2} min^{-1}. This type of fog collection system with a Janus membrane shows continuous condensation, collection, transfer and preserving functions and may provide a new way to harvest water from fog.

Conclusion

A facile single-layer hydrophobic/hydrophilic Janus aluminum membrane with dual gradient conical micropore arrays for efficient fog collection was fabricated by femtosecond laser drilling and subsequent selective surface modification. Compared with superhydrophilic membranes, the Janus membrane showed 209% enhancement and 75% decreased re-evaporation rate in fog collection. Furthermore, the distinctive morphology of conical pores and unique wetting produced the self-driving force, which could efficiently transfer the collected water from the top surface to the bottom one. This novel design of a Janus fog collection system with high-efficiency self-driving fog collection will provide a promising way for solving the water crisis and other industrial applications.

Conflicts of interest

There are no conflicts to declare.

Acknowledgements

References

1 H. Zhu, Z. G. Guo and W. M. Liu, Biomimetic water-collecting materials inspired by nature, *Chem. Commun.*, 2016, **52**, 3863–3879.

2 A. R. Parker and C. R. Lawrence, Water capture by a desert beetle, *Nature*, 2001, **414**, 33–34.

3 T. Xu, Y. C. Lin, M. X. Zhang, W. W. Shi and Y. M. Zheng, High-efficiency fog collector: water unidirectional transport on heterogeneous rough conical wires, *ACS Nano*, 2016, **10**, 10681–10688.

4 J. Ju, H. Bai, Y. M. Zheng, T. Y. Zhao, R. C. Fang and L. Jiang, A multi-structural and multi-functional integrated fog collection system in cactus, *Nat. Commun.*, 2012, **3**, 1247.

5 H. Bai, J. Ju, R. Z. Sun, Y. Chen, Y. M. Zheng and L. Jiang, Controlled fabrication and water collection ability of bioinspired artificial spider silks, *Adv. Mater.*, 2011, **23**, 3708–3711.

6 X. L. Tian, Y. Chen, Y. M. Zheng, H. Bai and L. Jiang, Controlling water capture of bioinspired fibers with hump structures, *Adv. Mater.*, 2011, **23**, 5486–5491.

7 H. Bai, R. Z. Sun, J. Ju, X. Yao, Y. M. Zheng and L. Jiang, Large-scale fabrication of bioinspired fibers for directional water collection, *Small*, 2011, **7**, 3429–3433.

This journal is © The Royal Society of Chemistry 2017

J. Mater. Chem. A, 2017, **5**, 18403–18408 | **18407**

8 H. Bai, J. Ju, Y. M. Zheng and L. Jiang, Functional fibers with unique wettability inspired by spider silks, *Adv. Mater.*, 2012, **24**, 2786–2791.

9 M. Y. Cao, J. S. Xiao, C. M. Yu, K. Li and L. Jiang, Hydrophobic/hydrophilic cooperative Janus system for enhancement of fog collection, *Small*, 2015, **11**, 4379–4384.

10 K. J. Ji, J. Zhang, J. Chen, G. Y. Meng, Y. F. Ding and Z. D. Dai, Centrifugation-assisted fog-collecting abilities of metal-foam structures with different surface wettabilities, *ACS Appl. Mater. Interfaces*, 2016, **8**, 10005–10013.

11 J. L. Yong, F. Chen, Q. Yang and X. Hou, Femtosecond laser controlled wettability of solid surfaces, *Soft Matter*, 2015, **11**, 8897–8906.

12 J. W. B. Bush, F. Peaudecerf, M. Prakash and D. Quéré, On a tweezer for droplets, *Adv. Colloid Interface Sci.*, 2010, **161**, 10–14.

13 X. Y. Ma, M. Y. Cao, C. Teng, H. Li, J. S. Xiao, K. S. Liu and L. Jiang, Bio-inspired humidity responsive switch for directional water droplet delivery, *J. Mater. Chem. A*, 2015, **3**, 15540–15545.

14 Y. M. Hou, M. Yu, X. M. Chen, Z. K. Wang and S. H. Yao, Recurrent filmwise and dropwise condensation on a beetle mimetic surface, *ACS Nano*, 2014, **9**, 71–81.

15 L. Zhai, M. C. Berg, F. Ç. Cebeci, Y. S. Kim, J. M. Milwid, M. F. Rubner and R. E. Cohen, Patterned superhydrophobic surfaces: toward a synthetic mimic of the Namib desert beetle, *Nano Lett.*, 2006, **6**, 1213–1217.

16 Q. B. Wang, X. Yao, H. Liu, D. Quéré and L. Jiang, Self-removal of condensed water on the legs of water striders, *Proc. Natl. Acad. Sci. U. S. A.*, 2015, **112**, 9247–9252.

17 H. Bai, X. L. Tian, Y. M. Zheng, J. Ju, Y. Zhao and L. Jiang, Direction controlled driving of tiny water drops on bioinspired artificial spider silks, *Adv. Mater.*, 2010, **22**, 5521–5525.

18 Y. Chen, L. Wang, Y. Xue, L. Jiang and Y. M. Zheng, Bioinspired tilt-angle fabricated structure gradient fibers: micro-drops fast transport in a long-distance, *Sci. Rep.*, 2013, **3**, 2927.

19 J. W. Chen, Y. M. Liu, D. W. Guo, M. Y. Cao and L. Jiang, Under-water unidirectional air penetration via a Janus mesh, *Chem. Commun.*, 2015, **51**, 11872–11875.

20 Z. J. Wang, Y. Wang and G. J. Liu, Rapid and efficient separation of oil from oil-in-water emulsions using a Janus cotton fabric, *Angew. Chem., Int. Ed.*, 2016, **128**, 1313–1316.

21 Z. J. Wang, G. J. Liu and S. S. Huang, In situ generated Janus fabrics for the rapid and efficient separation of oil from oil-in-water emulsions, *Angew. Chem., Int. Ed.*, 2016, **128**, 14830–14833.

22 X. L. Tian, H. Jin, J. Sainio, R. H. A. Ras and O. Ikkala, Droplet and fluid gating by biomimetic Janus membranes, *Adv. Funct. Mater.*, 2014, **24**, 6023–6028.

23 M. B. Wu, H. C. Yang, J. J. Wang, G. P. Wu and Z. K. Xu, Janus membranes with opposing surface wettability enabling oil-to-water and water-to-oil emulsification, *ACS Appl. Mater. Interfaces*, 2017, **9**, 5062–5066.

24 H. C. Yang, J. W. Hou, V. Chen and Z. K. Xu, Janus membranes: exploring duality for advanced separation, *Angew. Chem., Int. Ed.*, 2016, **55**, 13398–13407.

25 S. N. Zhang, J. Y. Huang, Z. Chen and Y. K. Lai, Bioinspired special wettability surfaces: from fundamental research to water harvesting applications, *Small*, 2017, **13**, 1602992.

26 G. Q. Li, H. Fan, F. F. Ren, C. Zhou, Z. Zhang, B. Xu, S. Z. Wu, Y. L. Hu, W. L. Zhu, J. W. Li, Y. S. Zeng, X. H. Li, J. R. Chu and D. Wu, Multifunctional ultrathin aluminum foil: oil/water separation and particle filtration, *J. Mater. Chem. A*, 2016, **4**, 18832–18840.

27 M. X. Zhang, L. Wang, Y. P. Hou, W. W. Shi, S. L. Feng and Y. M. Zheng, Controlled Smart Anisotropic Unidirectional Spreading of Droplet on a Fibrous Surface, *Adv. Mater.*, 2015, **27**, 5057–5062.

28 M. Prakash, D. Quéré and J. W. M. Bush, Surface tension transport of prey by feeding shorebirds: the capillary ratchet, *Science*, 2008, **320**, 931–934.

29 É. Lorenceau and D. Quéré, Drops on a conical wire, *J. Fluid Mech.*, 2004, **510**, 29–45.

18408 | *J. Mater. Chem. A*, 2017, **5**, 18403–18408

This journal is © The Royal Society of Chemistry 2017